JOURNAL OF MATERIALS SCIENCE 20 (1985) 4155–4162

# Quenched metastable phases and their transformations on heating in the $Bi_2O_3$–$WO_3$ system

TAKEYUKI SUZUKI, TSUTOMU YAMAZAKI, EIJI HOSAKA, HIROSHI YOSHIOKA
*Department of Industrial Chemistry, Tokyo University of Agriculture and Technology, Koganeishi, Tokyo 184, Japan*

A single-roller apparatus was used to quench 16 melts in the $Bi_2O_3$–$WO_3$ system. Metastable polycrystalline phases were obtained in all compositions. Quenched specimens and their phase transformations on heating were examined by X-ray diffraction, differential thermal analysis, density measurement, electrical measurement and observation of optical anisotropy. Fcc solid solutions of the type, $2WO_3 \rightarrow 2W_{Bi}^{\cdots} + 3O_{\square}'' + 3O_O^x$ occurred in the quenched samples for 18 to 32 mol% $WO_3$. Quenched phases remained unchanged with only a slight structural relaxation at temperatures lower than the first exotherm. Near the first exotherm, most samples showed an irregular change in the lattice parameter(s).

## 1. Introduction

In our previous studies [1, 2], the occurrence and properties of melt-quenched solid solutions in the system $Bi_2O_3$–$MoO_3$ were reported. Such solid solutions showed the potential for yielding high oxide ion conductors at temperatures lower than the 600° C or so limit of stabilized zirconias. Of particular interest to us was the observation that the solid electrolyte cell based on this quenched film showed attractive properties as an oxygen sensor at temperatures as low as 350° C [3]. However, the quenched solid solution was metastable, thus causing phase transitions on heating, which discouraged the use of the quenched metastable film (face centred cubic structure, 16 mol% $MoO_3$ sample). This observation prompted a selection of oxide additives and a study of phase transitions on heating so that the resulting quenched or annealed samples may show an improved stability. Thus, binary systems of $Bi_2O_3$ presenting congruent melting compounds with face centred cubic (fcc) structure were surveyed and tungsten trioxide was chosen. The $Bi_2O_3$–$WO_3$ system interests us not only for the occurrence of the congruent melting compound $Bi_6WO_{12}$ [4], but also for its high oxide ion conductivity observed in the sintered samples [5], in addition to the similarity in the crystal chemistry of tungsten to molybdenum. In this report we describe the occurrence of quenched phases in the system $Bi_2O_3$–$WO_3$, their characterization by X-ray diffraction (XRD), differential thermal analysis (DTA), density measurement, electrical data and some observations on the nature of the phase transition paths on heating.

## 2. Experimental methods

Samples were prepared from $Bi_2O_3$ (99.9%) and $WO_3$ (99.9%) powders by mixing and melt-quenching in the single-roller apparatus. Details of roller-quenching, examination by XRD and measurement of conductivity by the complex impedance method have been described previously [1–3]. Initially, samples were prepared at 4 mol% intervals up to 40 mol% $WO_3$, with intermediate compositions as needed. Some samples having the same compositions as the quenches were made, in some instances by slower cooling from the melts or by sintering.

0022–2461/85 $03.00 + .12  

Quenched materials were examined first by polarizing microscopy and then X-rayed to determine the crystal structure. When optical anisotropy was observed, the ratio of polarizing areas to the total area was estimated visually. Relative amount of coexisting $\beta$-phase in the $\delta$-phase matrix, for example, was also estimated from the peak heights, $I(h\,k\,l)$, in the XRD chart by the formula:

$$\frac{\sum I(h\,k\,l)_\beta}{\sum I(h\,k\,l)_\delta + \sum I(h\,k\,l)_\beta}$$

These values should be considered as only tentative in the absence of detailed polarization and XRD interpretations. DTA was conducted in platinum cups in the high-temperature cell of a thermoanalyser (Rigaku: thermoflex) at 10 K $min^{-1}$ in air. Transition temperatures were recorded as the extrapolated onset of each peak. Some samples were subsequently heated to various temperatures in open platinum crucibles or DTA cups and X-rayed at room temperature to observe the change in crystal structure.

The density was measured by pycnometry using *n*-butanol as the immersion medium; reduced atmospheric pressure, achieved using a rotary pump, facilitated an extraction of gaseous inclusions at the liquid–sample interface. Reweighing after melting showed losses of $< 0.3\%$; these small losses were neglected and the nominal compositions are used throughout this work.

## 3. Results and discussion

### 3.1. Quenched materials

The resulting polycrystalline samples were generally thin films, typically 15 $\mu$m × 1 mm × 20 mm in size. The compositions having 36 and 40 mol % $WO_3$ were the exceptions; they were almost flake-like powders. All compositions tried and phases encountered are given in Table I. A comparison with literature data in quenched pure $Bi_2O_3$ gives a rough estimation of the present cooling rate. Sarjeant and Roy [6] reported that the single tetragonal ($\beta$) phase (JCPDS No. 18-244) could be retained by using splat-quench technique with a glass slide as a substrate or even an injection of molten drops into ionized water by the Verneuil crystal-growing apparatus yielded the same phase, whereas our quenches were the mixtures of the tetragonal ($\beta$) phase (JCPDS No. 27-50) and the monoclinic ($\alpha$) phase (JCPDS No. 27-53). Since the $\alpha$-$Bi_2O_3$ is the low-temperature polymorph, these observations indicate that our single-roller quenching provides a lower quenching rate, probably $10^4$ to $10^5$ K $sec^{-1}$. In fact, melts were instantly driven off from the rotating disc with no evidence of wetting of the metal disc; these resulted in poor heat transfer.

In the single-roller quenching, melts are unidirectionally solidified and this causes preferred crystallographic orientations. The orientation degrees parallel to the film thickness are given in the last column of Table I. These are derived from the XRD analyses assuming no preferred orientation for finely ground films [7]. It is indicated that the $\langle 1\,1\,1 \rangle$ direction is almost parallel to the film thickness in compositions where fcc ($\delta$) phase is dominant.

Results of DTA on ground films were next examined. DTA was conducted up to 800° C for 0 to 14 mol % and 950° C for 16 to 40 mol % $WO_3$; there was often more than one exotherm (e.g. pure $Bi_2O_3$, 8 and 18 mol % $WO_3$) or no exotherm at all (e.g. 16 mol % $WO_3$). All exotherms were found to be irreversible for their absence on re-heating, whereas all endotherms were reversible. Transition temperatures together with the results of XRD are given in Fig. 1, where four isotherms corresponding apparently to those given in the phase diagram by Speranskaya [4] are drawn. It is evident that samples are in equilibrium at temperatures at least above ~700° C. At temperatures lower than the first exotherms, quenched phases remained unchanged with only a slight structural relaxation (as will be seen later) under the present DTA conditions. Detailed transformation sequences at low and intermediate temperatures are discussed later for some selected compositions.

Note that Nassau *et al.* [8] termed a diagram similar to Fig. 1 a "metastable phase transformation diagram" to indicate its limitation.

Leaving aside the structural aspect for the moment, let us now look at the electrical conductivity. The complex impedance parallel to the film plane was determined in air over the frequency range ~1 Hz to 100 kHz. Typical impedance plots are shown in Fig. 2. The resistance values, and therefore conductivities, are derived from the circular-arc intercepts on the $Z'$-axis. Results are given in Fig. 3 as a function

TABLE I Quenched specimens in the $Bi_2O_3$–$WO_3$ system

| $WO_3$ (mol %) | Colour | Polarization (%) | Phase (%) | Direction and orientation degree (%)* |
|---|---|---|---|---|
| 0 | orange, opaque | 100 | $\beta^{\dagger} + \alpha^{\ddagger}$ (10) | – |
| 4 | yellowish orange, transparent | 100 | $\beta$ | $c$-axis (20) |
| 8 | reddish yellow, transparent | < 0.1 | $\delta^{\S} + \beta$ (20) | – |
| 12 | dull yellow, transparent | < 0.1 | $\delta + \beta$ (15) | ⟨1 1 1⟩ (40) |
| 14, 16 | pale yellow, transparent | < 0.1 | $\delta + \beta$ (5) | ⟨1 1 1⟩ (80) for 16 mol % |
| 18, 20, 22, 24, 25 | pale yellow, transparent | 0 | $\delta$ | ⟨1 1 1⟩ (80) for 20 and 24 mol % |
| 26, 28 | yellowish gray, transparent | 0 | $\delta$ | ⟨1 1 1⟩ (70) for 28 mol % |
| 32 | pale yellow, transparent | 0 | $\delta$ | ⟨1 1 1⟩ (70) |
| 33.3 | pale yellowish brown, transparent | 20 | $\delta + \gamma^{\P}$ (10) | – |
| 36 | pale yellow, opaque | 40 | $\delta + \gamma$ (20) | – |
| 40 | yellow, opaque | 40 | $\delta + \gamma$ (50) | – |

*Orientation along the film thickness.
†Tetragonal (JCPDS No. 27-50).
‡Monoclinic (JCPDS No. 27-53).
§Fcc, see [10].
¶Orthorhombic, see [11].

of composition and temperature. These were measured in the heating-up direction at an average rate of $\sim 1\,K\,min^{-1}$. It is possible that this low heating rate, as against the $10\,K\,min^{-1}$ of the DTA, has induced lower transition temperatures than those indicated in Fig. 1. Indeed the 28 mol % $WO_3$ sample, for instance, showed an irregular conductivity behaviour at temperatures as low as $\sim 500°$ C which is considerably lower than the expected transition temperature of $\sim 620°$ C.

However, occurrence of a transition with little heat liberation, thus not detected by the DTA, but a large change in conductivity cannot, of course, be ruled out. Some examples are discussed later.

The conductivities of the 28 mol % $WO_3$ sample are $7.1 \times 10^{-2}$, $1.4 \times 10^{-2}$, $1.5 \times 10^{-2}$, $2.2 \times 10^{-3}$ and $2.8 \times 10^{-4}\,(\Omega\,cm)^{-1}$ at 700, 600, 500, 400 and 300° C, respectively. These values are considerably higher than those of stabilized zirconias and almost the same as those found for sintered samples by Takahashi and Iwahara [5].

Further studies on oxide ion conduction are in progress.

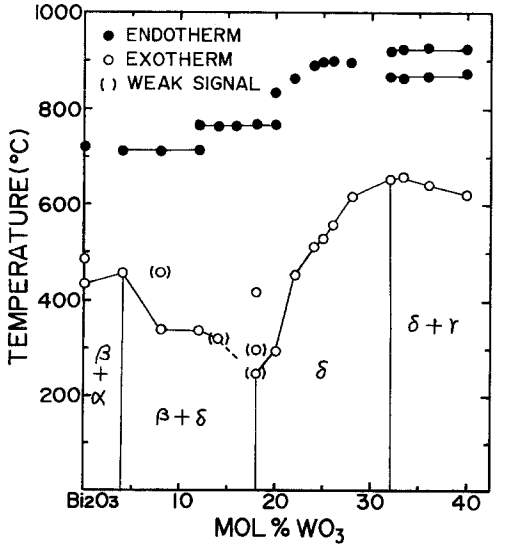


*Figure 1* Transformation of quenched phases in the $Bi_2O_3$–$WO_3$ system. Samples are heated at $10\,K\,min^{-1}$.

## 3.2. Fcc ($\delta$) solid solution

From 8 to 36 mol % $WO_3$ predominant fcc ($\delta$) phase was observed by XRD, of which 18 to 32 mol % $WO_3$ samples were pure fcc in terms of both optical isotropy and XRD identification. This pure form gave an increasing exothermic temperature with the content of $WO_3$ (Fig. 1). The observed lattice constants given in Fig. 4 decreased with $WO_3$. This decrease forms a striking contrast to the metastable fcc ($\delta$) phase in the system $Bi_2O_3$–$MoO_3$; our previous work [2] revealed an increasing lattice constant with an increasing $MoO_3$ content (4 to 16 mol % $MoO_3$). The difference is rather surprising in view of the similarity of tungsten to molybdenum; both elements are located in the same column on the Periodic Table and both have almost identical ionic radii and electronegativities. Thus formation of the fcc solid solutions was investigated further; calculated and measured densities were compared to interpret

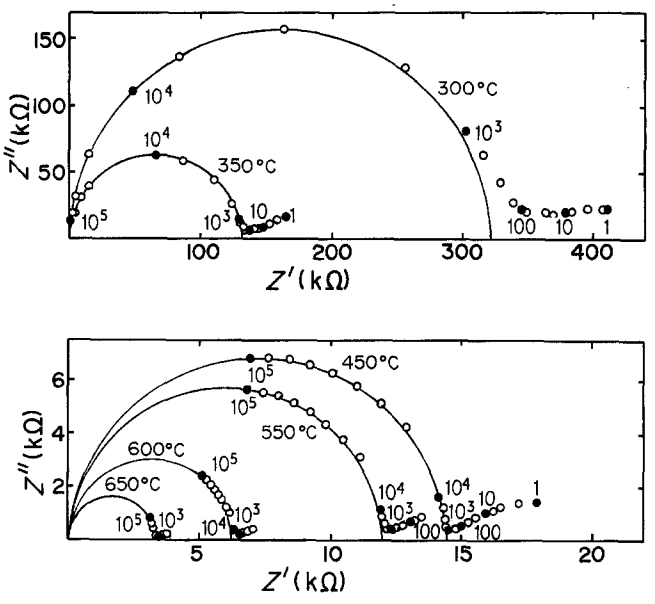


*Figure 2* Typical impedance plots for 28 mol % $WO_3$ sample. Frequencies are marked in Hz.

the incorporation of $WO_3$ into $Bi_2O_3$. The first step is to construct typical defect models. When $WO_3$ forms a solid solution with $Bi_2O_3$, a general formation reaction can be expressed using Kröger–Vink notation [9] as:

$$WO_3 \rightarrow aW_{Bi}^{\cdots} + bW_i^{\cdots\cdots} + cV_{Bi}^{'''} + dO_{\square}'' + eO_O^x$$

where $\square$ denotes an oxide ion vacancy. Mass and charge balance require the following relationship:

$$1 = a + b,\ 3 = d + e,\ 3a + 6b = 3c + 2d$$

The original unit cell of the pure fcc ($\delta$) $Bi_2O_3$ may be expressed as $Bi_4O_6\square_2$ [10]. Taking account of the cationic lattice number 4 and the decrease in the number of $\square$ with the formation of $O_{\square}''$, the unit cell formula of the composition $(Bi_2O_3)_{1-x}(WO_3)_x$ is given by:

$$Bi_{8(1-x)/g}W_{4x/g}O_{12/g}\square_{4(1-x-dx)/g}$$

where $x$ is the mole fraction and $g = 2 - (2 - a - c)x$. Seven simple models and the corresponding unit cell formulae are given in

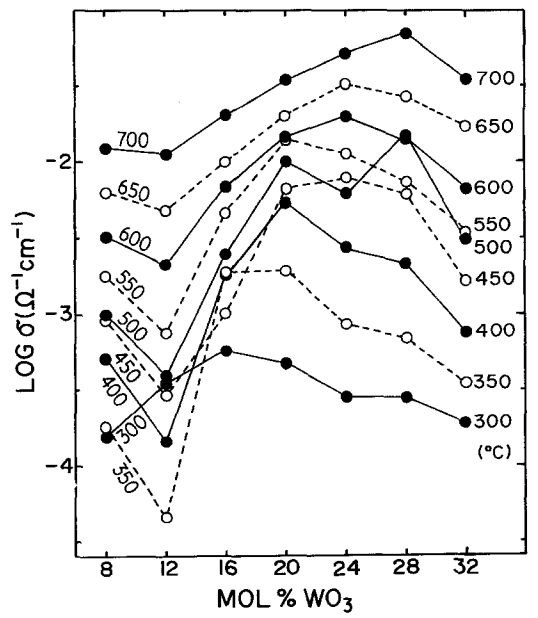


*Figure 3* Conductivity isotherms taken in the heating-up direction at ~ 1 K $min^{-1}$.

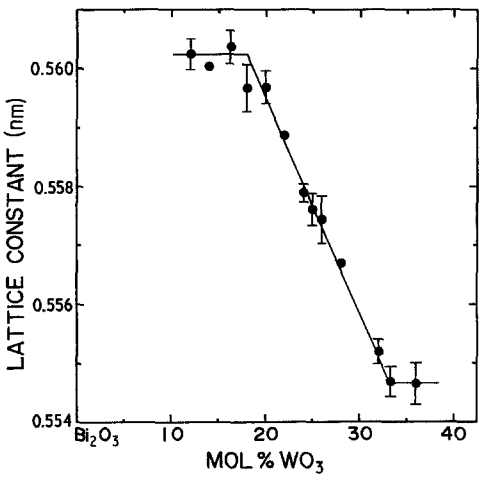


*Figure 4* Lattice parameters of fcc ($\delta$) phase in the quenched $Bi_2O_3$–$WO_3$ system.

TABLE II Typical reaction model and unit cell formula

| Model | Formation reaction | Unit cell formula |
|---|---|---|
| 1 | $WO_3 \rightarrow W_i^{\cdots\cdots} + 3O_{\square}''$ | $Bi_4W_{2x/(1-x)}O_{6/(1-x)}\square_{2(1-4x)/(1-x)}$ |
| 2 | $6WO_3 \rightarrow 2W_{Bi}^{\cdots} + 4W_i^{\cdots\cdots} + 15O_{\square}'' + 3O_O^X$ | $Bi_{24(1-x)/(6-5x)}W_{12x/(6-5x)}O_{36/(6-5x)}\square_{6(2-7x)/(6-5x)}$ |
| 3 | $3WO_3 \rightarrow 2W_{Bi}^{\cdots} + W_i^{\cdots\cdots} + 6O_{\square}'' + 3O_O^X$ | $Bi_{12(1-x)/(3-2x)}W_{6x/(3-2x)}O_{18/(3-2x)}\square_{6(1-3x)/(3-2x)}$ |
| 4 | $2WO_3 \rightarrow 2W_{Bi}^{\cdots} + 3O_{\square}'' + 3O_O^X$ | $Bi_{8(1-x)/(2-x)}W_{4x/(2-x)}O_{12/(2-x)}\square_{2(2-5x)/(2-x)}$ |
| 5 | $3WO_3 \rightarrow 3W_{Bi}^{\cdots} + V_{Bi}''' + 3O_{\square}'' + 6O_O^X$ | $Bi_{12(1-x)/(3-x)}W_{6x/(3-x)}O_{18/(3-x)}\square_{6(1-2x)/(3-x)}$ |
| 6 | $6WO_3 \rightarrow 6W_{Bi}^{\cdots} + 4V_{Bi}''' + 3O_{\square}'' + 15O_O^X$ | $Bi_{24(1-x)/(6-x)}W_{12x/(6-x)}O_{36/(6-x)}\square_{6(2-3x)/(6-x)}$ |
| 7 | $WO_3 \rightarrow W_{Bi}^{\cdots} + V_{Bi}''' + 3O_O^X$ | $Bi_{4(1-x)}W_{2x}O_6\square_{2(1-x)}$ |

Table II. These unit cell formulae when combined with the measured lattice constants (Fig. 4) readily yield calculated densities. Calculated and measured densities are compared in Fig. 5. This figure shows that the incorporation of $WO_3$ into $Bi_2O_3$ can best be approximated by the model 4, that is, formation of the substitutional solid solution. According to this model the number of oxide ion vacancies $\square$ per unit cell decreases from 1.21 at $x = 0.18$ to 0.48 at $x = 0.32$. It is to be noted that the fcc ($\delta$) quenches of the system $Bi_2O_3$–$MoO_3$ formed also substitutional type solid solutions [2].

## 3.3. Phase transformation on heating

The five compositions (4, 16, 18, 25 and 33.3 mol % $WO_3$) were studied. The electrical resistances. $R$, were determined here at 1 kHz along the film plane; the heating rate used was 1 to 3 K $min^{-1}$. For comparison with the DTA data the relative values, $R_T/R_{300°C}$, are used since these do not miss, as the DTA sometimes does,

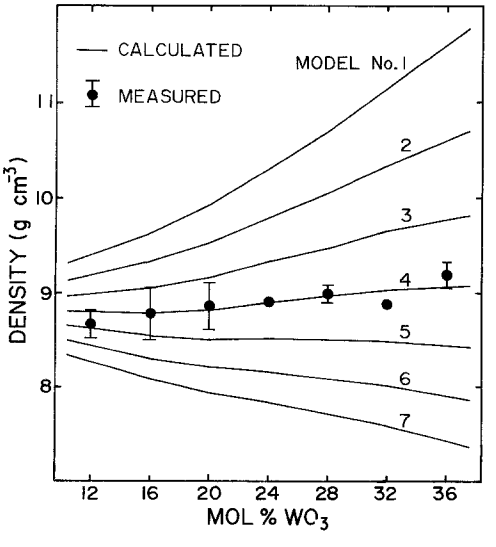


*Figure 5* Comparison of the calculated and measured density.

small structural changes sensitive to the electrical conduction.

### 3.3.1. 4 mol% $WO_3$ (Fig. 6)

Quenched pure tetragonal ($\beta$) phase transformed to the monoclinic ($\alpha$) phase at temperatures corresponding to the exotherm (455 to 494° C). X-ray examination revealed an increasing tendency in the $a$-lattice parameter from $a = 0.7737$ nm at 400° C to 0.7744 nm at 445° C and a gradual decrease in the other parameter from $c = 0.5661$ nm at room temperature to 0.5647 nm at 445° C. On further heating to 500, 600 or 700° C, the $\alpha$-phase replaced completely the $\beta$-phase. Most surprising was the observation that the polarizing area decreased to 75 to 90% in samples heated to 400 to 445° C. Optical isotropy occurred always at the circumferential region of the film. The only plausible interpretation lies in the development of the crystallographic orientation. In fact, the overall orientation degrees of the $c$-axis along the film thickness were found to be 40 and 30% at 400 and 445° C, respectively. These values are certainly larger than the 20% obtained in as-prepared samples (Table I). The resistance data showed no significant change around 450° C; the large change at about 550° C did not correspond to the DTA data.

### 3.3.2. 16 mol% $WO_3$ (Fig. 7)

This is the only composition which showed no exotherm. However, the resistance data clearly indicated some changes at 350 to 500° C. Quenched phases are mixtures of $\delta$- and $\beta$-phase. A sudden growth of the $\beta$-phase was observed on heating up to 350° C. At the same time, the lattice constant in the $\delta$-phase increased anomalously at 350 and 400° C. Heating to 500° C produced an unknown (?) phase; this phase was not investigated further. The $c$-parameter in the $\beta$-phase increased with

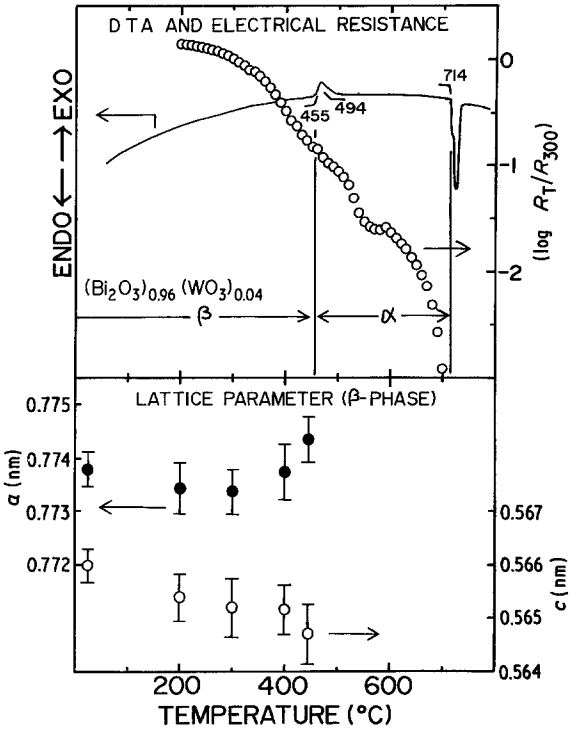


*Figure 6* Transition sequence of the 4 mol % $WO_3$ sample.

increasing temperature from 450 to 700° C, but the *c*- and *a*-parameters were somewhat irregular at 350 to 400° C. These variations in the crystal structures are in good agreement with the irregular behaviour in the resistance data.

### 3.3.3. 18 mol% $WO_3$ (Fig. 8)

This composition is the lower limit of the pure δ-phase. It showed three exotherms, two weak exotherms (248 to 274 and 298 to 331° C) and one distinct exotherm (420 to 465° C). A sudden increase in the lattice constant (δ-phase) was observed at 350 and 400° C; this behaviour was the same as that found in the 16 mol % $WO_3$ samples. Heating to 600 and 700° C produced the β-phase. Polarization was not observed for

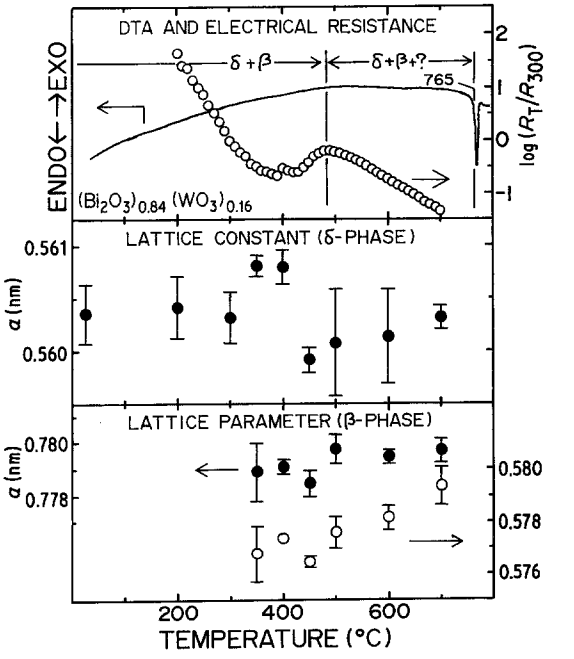


*Figure 7* Transition sequence of the 16 mol % $WO_3$ sample.

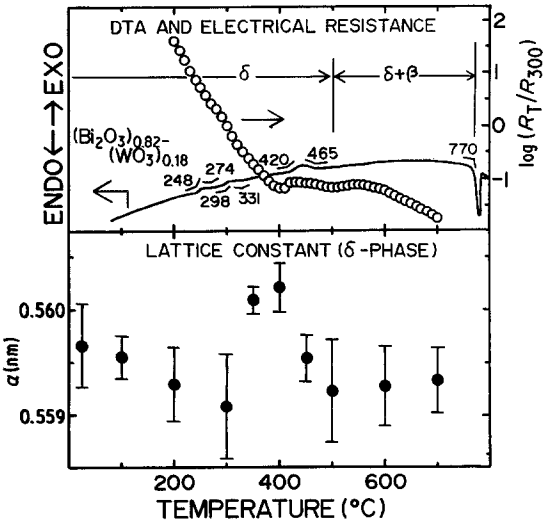


*Figure 8* Transition sequence of the 18 mol % $WO_3$ sample.

temperatures lower than 500° C, but samples heated up to 600 and 700° C showed a considerable amount of optical anisotropy due to the growth of the $\beta$-phase. Complicated variations in the resistance data were observed at 400 to 550° C; however, these variations could not be directly related to the change in the crystal structure.

### 3.3.4. 25 mol% $WO_3$ (Fig. 9)

This composition corresponds to the compound $Bi_6WO_{12}$ [4]. Quenched $\delta$-phase remained as it was with only a slight structural relaxation on heating up to 528° C. It is interesting to note that the structural relaxation, observed by the change in the lattice constant, has already begun at temperatures as low as 100 to 200° C. The same exotherm (530 to 576° C) as illustrated in Fig. 9 was observed for samples prepared by dropping the melts into liquid nitrogen or even on to a stainless steel plate kept at room temperature. Probably the cooling rate does not play an important role in retaining the $\delta$-phase. During and especially after the exotherm, the powder patterns showed a reduction of symmetry such as splitting of lines, but these changes were not investigated in the present study and these phases were treated as pseudo-cubic and designated $\delta'$. Neither the quenched phases nor the sintered samples produced the expected stable fcc phase [4, 5] on prolonged heating at 800 to 850° C. The knees in the resistance curve (480 to 520° C) probably correspond to the transformation $\delta \rightarrow \delta'$ (528° C) because the resistance was measured at a slower heating rate than that of the DTA.

### 3.3.5. 33.3 mol% $WO_3$ (Fig. 10)

This composition corresponds to the compound $Bi_4WO_9$ [4]. Quenched phases are mixtures of $\delta$- and $\gamma$-phase. On heating the sample showed an exotherm at 657 to 722° C, indicating the highest transition temperature among all compositions tested. Phases observed after the exotherm were also the mixtures of the same phases as before the exotherm. However, relative amounts of the $\gamma$-phase increased from 10% (600° C) to 35% (800° C) and at the same time the lattice constant of the $\delta$-phase increased remarkably from 0.5542 nm at 600° C to 0.5593 nm at 800° C. A large change in the resistance data around 620° C is probably due to the growth of the $\gamma$-phase.

## 4. Conclusions

1. Rapid-quenching of the melts in the system $Bi_2O_3$–$WO_3$ produced the tetragonal ($\beta$) phase at

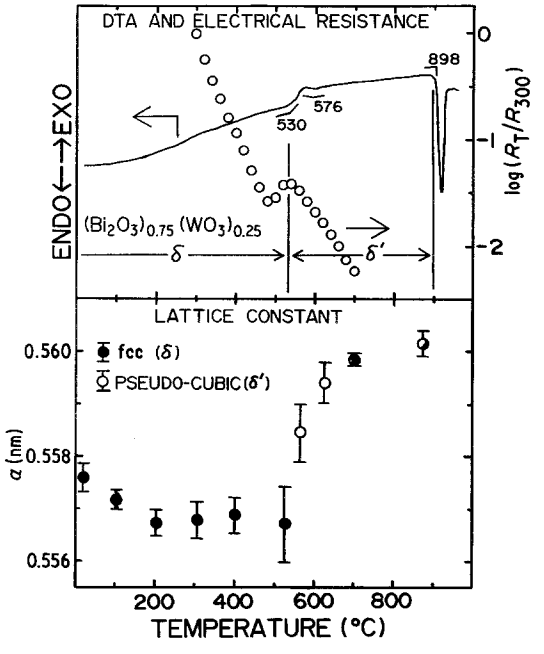


*Figure 9* Transition sequence of the 25 mol % $WO_3$ sample.

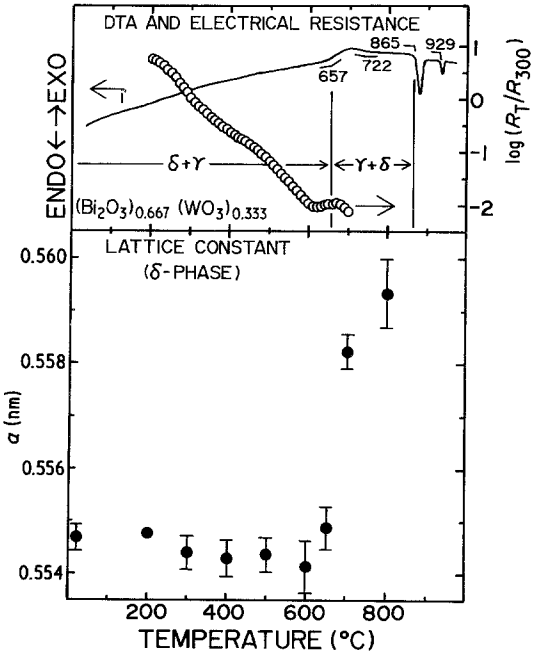


*Figure 10* Transition sequence of the 33.3 mol % $WO_3$ sample.

4 mol % $WO_3$ and the fcc ($\delta$) phase at 18 to 32 mol % $WO_3$.

2. Quenched phases remained unchanged with only a slight structural relaxation for temperatures lower than the first exotherm by DTA. Most samples showed an irregular change in the lattice parameter(s) near the first exotherm.

3. Substitutional solid solutions of the type $2WO_3 \rightarrow 2W_{Bi}^{\cdots} + 3O_{\square}^{''} + 3O_{O}^{x}$, occurred for the quenched fcc phase.

4. Transition temperature, indicated by the first exotherm, of the $\delta$-phase increased with the increase of the $WO_3$ content.

## References


1. T. SUZUKI and S. UKAWA, *J. Mater. Sci.* **18** (1983) 1845.
2. T. SUZUKI, S. UKAWA, M. MORITA and K. HOSHI, in Proceedings of the International Meeting on Chemical Sensors, Fukuoka, September 1983, edited by T. Seiyama, K. Fueki, J. Shiokawa and S. Suzuki (Kodansha/Elsevier, Tokyo, 1983) p. 256.
3. T. SUZUKI, K. KAKU, S. UKAWA and Y. DANSUI, *Solid State Ionics* **13** (1984) 237.
4. E. I. SPERANSKAYA, *Inorg. Mater.* **6** (1970) 127, (English translation).
5. T. TAKAHASHI and H. IWAHARA, *J. Appl. Electrochem.* **3** (1973) 65.
6. P. T. SARJEANT and R. ROY, *J. Amer. Ceram. Soc.* **50** (1967) 500.
7. F. K. LOTGERING, *J. Inorg. Nucl. Chem.* **9** (1959) 113.
8. K. NASSAU, C. A. WANG and M. GRASSO, *J. Amer. Ceram. Soc.* **62** (1979) 74.
9. F. A. KRÖGER, "The Chemistry of Imperfect Crystals", Vol. 2 (North-Holland, Amsterdam, 1974) p. 1.
10. L. G. SILLEN and B. AURIVILLIUS, *J. Kristallogr.* **101** (1939) 483.
11. E. L. GALIPERIN, L. Y. ERMAN, I. K. KOLCHIN, M. A. BELOVA and K. S. CHERNISHEV, *Zh. Neorg. Khim.* **11** (1966) 2195.



*Received 12 December 1984*
*and accepted 15 January 1985*